

# Assessing the effectiveness of the intervention measures of COVID-19 in China based on dynamical method

Xiaomeng Wei <sup>a, b, c</sup>, Mingtao Li <sup>d</sup>, Xin Pei <sup>d</sup>, Zhiping Liu <sup>e</sup>, Juan Zhang <sup>a, b, \*</sup>

<sup>a</sup> Complex Systems Research Center, Shanxi University, 030006, Shanxi, China

<sup>b</sup> Shanxi Key Laboratory of Mathematical Techniques and Big Data Analysis on Disease Control and Prevention, 030006, Shanxi, China

<sup>c</sup> School of Mathematical Sciences, Shanxi University, 030006, Shanxi, China

<sup>d</sup> College of Mathematics, Taiyuan University of Technology, 030024, Shanxi, China

<sup>e</sup> School of Data Science and Technology, North University of China, 030051, Shanxi, China

## ARTICLE INFO

### Article history:

Received 31 October 2022

Received in revised form 29 December 2022

Accepted 29 December 2022

Available online 5 January 2023

Handling Editor: Dr. Eftimie Raluca

### Keywords:

COVID-19

Close contact tracking

Large-scale nucleic acid testing

Dynamics

The basic reproduction number

Sensitivity analysis

## ABSTRACT

Normalized interventions were implemented in different cities in China to contain the outbreak of COVID-19 before December 2022. However, the differences in the intensity and timeliness of the implementations lead to differences in final size of the infections. Taking the outbreak of COVID-19 in three representative cities Xi'an, Zhengzhou and Yuzhou in January 2022, as examples, we develop a compartmental model to describe the spread of novel coronavirus and implementation of interventions to assess concretely the effectiveness of Chinese interventions and explore their impact on epidemic patterns. After applying reported human confirmed cases to verify the rationality of the model, we apply the model to speculate transmission trend and length of concealed period at the initial spread phase of the epidemic (they are estimated as 10.5, 7.8, 8.2 days, respectively), to estimate the range of basic reproduction number (2.9, 0.7, 1.6), and to define two indexes (transmission rate  $v_t$  and controlled rate  $v_c$ ) to evaluate the overall effect of the interventions. It is shown that for Zhengzhou,  $v_c$  is always more than  $v_t$  with regular interventions, and Xi'an take 8 days to achieve  $v_c > v_t$  twice as long as Yuzhou, which can interpret the fact that the epidemic situation in Xi'an was more severe. By carrying out parameter values, it is concluded that in the early stage, strengthening the precision of close contact tracking and frequency of large-scale nucleic acid testing of non-quarantined population are the most effective on controlling the outbreaks and reducing final size. And, if the close contact tracking strategy is sufficiently implemented, at the late stage large-scale nucleic acid testing of non-quarantined population is not essential.

© 2023 The Authors. Publishing services by Elsevier B.V. on behalf of KeAi Communications Co. Ltd. This is an open access article under the CC BY-NC-ND license (<http://creativecommons.org/licenses/by-nc-nd/4.0/>).

## 1. Introduction

The COVID-19 which was first reported in Wuhan city, Hubei province, China (Hui et al., 2020) in December 2019 spread so rapidly among people around the world that it has been characterized as pandemic by the World Health Organization

\* Corresponding author. Complex Systems Research Center, Shanxi University, 030006, Shanxi, China.

E-mail address: [zhangjuan1020@sxu.edu.cn](mailto:zhangjuan1020@sxu.edu.cn) (J. Zhang).

Peer review under responsibility of KeAi Communications Co., Ltd.

(WHO)([World Health Organization, 2020](#)). As of October 2022, the epidemic is spreading faster and faster and has intensified with time as new strains constantly appeared. It has infected over 615 million confirmed cases ([World Health Organization, 2022](#)) and caused incalculable damage to the international community.

In the face of the Wuhan epidemic, timely preventive and control measures that mainly included physical isolation were taken by China and they succeeded in managing the outbreak. Subsequently, the epidemiological management in China was improved and regular prevention and control measures were developed, then the government gradually explored its dynamic zero-COVID policy ([Chinese State Council, 2020](#)). With the guidance of dynamic zero-COVID policy, many times of the local outbreaks on the mainland were eliminated time and time again.

Meanwhile, the risk of clusters of epidemics remain in China due to the repeated shocks of COVID-19. In particular, considerable movement of people makes it more difficult to prevent and control the epidemic during holiday periods. In December 2021, approaching New Year and Spring Festival, Xi'an city in Shaanxi Province even experienced the largest outbreak in clusters since the outbreak in Wuhan. The number of confirmed cases went as high as 2053, which lasted for 43 days ([Health Commission of Shaanxi province, 2022](#)). Soon after, two local outbreaks occurred in Zhengzhou and Yuzhou of Henan Province, respectively. The detailed situations of three outbreaks are given as follows: For the epidemic situation in Xi'an, there are three known chains of transmission, the first two of which were detected in its early stage and did not cause the spread of the epidemic. The third chain of transmission was the focused flashpoint of that round of the epidemic in Xi'an. The first two cases of the third chain of transmission were a college teacher and his wife's mother, who had driven to Xi'an Xianyang International airport on December 4. On December 14, they were tested positive for the coronavirus. Subsequently, some of his colleagues were diagnosed successively with COVID-19 and had led to the local outbreak of COVID-19 in Xi'an. Meanwhile, on December 18 officials drew an elementary conclusion that the outbreak derived from imported cases on flight from Pakistan to Xi'an on December 4th, which was formally determined on January 7, 2022. On December 15, the relevant departments rapidly conducted epidemiological investigations, close and indirect contacts were placed in centralized quarantines and corresponding communities were in lockdown. However, there were still the infected individuals outside the Lockdown Zone. On December 23, the whole city adopted close management and large-scale nucleic acid testing of non-quarantined population, then the potential sources of infection were found and the epidemic situation was held down. As of January 21, 2022, the number of new cases was reported as zero. Xi'an was lifted lockdown and people got back to a normal life on January 24. Unfortunately, on January 2, 2022, a handyman of a ceramic enterprise in Yuzhou, Henan province, was found to be infected with SARS-CoV-2 when he went to the hospital for examination of other diseases. An old lady in Zhengzhou, Henan province, was tested positive for SARS-CoV-2 when taking a routine nucleic acid testing for hospitalization due to other reasons on Jan 3. Genetic sequencing showed that the strains types of viruses in Zhengzhou and Yuzhou were homologous, but the source of the viruses was still unknown. The double centers of spreading between the two cities were formed in that round of epidemic in Henan Province. Neither outbreak spilled over to other regions, and most cases in Yuzhou were found within regions that were managed early. By triggering a series of emergency action, the outbreaks in these two cities in Henan province, where the number of new infections returned to zero on January 20, were all brought under control in less than 20 days. The total number of confirmed cases were 135 and 365 in Zhengzhou and Yuzhou, respectively ([Health Commission of Henan province, 2022](#)). The three cities curbed the epidemics spread by taking regular measures, and achieved the aim of wiping out the epidemic at last. But the final number of infections, the duration of the epidemic and so on varied a great deal. Compared with the Xi'an, the outbreaks in Zhengzhou and Yuzhou lasted for a relatively short time and had smaller final size of the infections. To achieve Zero-COVID Status of high quality and explore the causes of large-scale outbreaks, we will apply mathematical models to quantificationally assess the effectiveness of the intervention measures taking these three local outbreaks for examples.

In view of the COVID-19 pandemic, many domestic and international scholars have already investigated and reported from all aspects such as mathematical modeling ([Majumder et al., 2022](#); [Rai et al., 2022](#); [Song et al., 2020, 2021](#); [Sun et al., 2022](#); [Wang et al., 2020](#); [Zhao et al., 2021](#)), epidemiology ([Qi & Yu, 2020](#)), and virologists ([Ceraolo & Giorgi, 2020](#)). Among mathematical modeling, dynamical model is one effective mechanism method and plays an important role in estimating the effect of measures adopted against outbreaks. One of the most widely used models in COVID-19 research is SEIR model ([Sun et al., 2020](#); [Tang et al., 2020](#)). Based on different research purposes, some researchers also extended the conventional SEIR model ([Biala et al., 2022](#); [Khairulbahri, 2021](#); [Kondo, 2021](#); [Liu et al., 2022](#); [Maged et al., 2022](#); [Rai et al., 2022](#); [Saadatmand et al., 2022](#); [Tiwarei et al., 2021](#); [Wang et al., 2021](#); [Yu et al., 2021](#); [Zhang et al., 2022](#)) to follow the intervention processes in different regions. Some of studies focused on the efficiency of single intervention, such as mask-wearing ([Maged et al., 2022](#)), restrictions on interregional movement ([Kondo, 2021](#)), contact tracing ([Biala et al., 2022](#)) and social media advertisements ([Rai et al., 2022](#); [Tiwarei et al., 2021](#)). Some took a single outbreak as the research object to assess the effectiveness of interventions ([Liu et al., 2022](#); [Saadatmand et al., 2022](#); [Wang et al., 2021](#)). Some analyzed the importance of measures to control COVID-19 spread by comparing the COVID-19 flow in different countries ([Khairulbahri, 2021](#); [Yu et al., 2021](#); [Zhang et al., 2022](#)). In this paper, we evaluate the effectiveness of the interventions by analyzing COVID-19 spread in different regions of the country with the same control measures, taking Xi'an, Zhengzhou and Yuzhou as examples. Aimed at the Xi'an outbreak, Yang et al. ([Yang et al., 2022](#)) evaluated the effects of managing population movement by simulating the epidemic trend in Xi'an under three scenarios of limited population movement. For epidemics in Zhengzhou and Yuzhou in January 2022, there are almost no research up to present.

In this paper, we take the transmission of COVID-19 epidemics in Xi'an, Zhengzhou and Yuzhou as three representative areas. The local governments adopted similar preventive and control measures with different efficiency and capacity: taking

large-scale nucleic acid testing of non-quarantined population, accurately tracing close contacts and secondary contacts, and management of people at high risk, etc. To assess the effects of control measures, we apply dynamics to compare transmission of COVID-19 in the three regions. The rest of this article is organized as follows: in Section 2, a COVID-19 dynamical model with interventions is established and we derive the expressions for the basic reproduction number, transmission rate and controlled rate. We apply public information and data to verify the rationality of the model, carry out the analysis of sensitivity for key parameters and assess and compare the impact of interventions on the spread of COVID-19 in three cities in Section 3. Section 4 gives the discussion and conclusion.

## 2. Material and methods

### 2.1. Materials

The data on COVID-19 human cases from December 9, 2021 to January 20, 2022 in Xi'an comes from the Health Commission of Shaanxi Province ([Health Commission of Shaanxi province, 2022](#)), and data from January 2 to January 19, 2022 in Yuzhou, and data from January 3 to January 19, 2022 in Zhengzhou are obtained from the Health Commission of Henan Province ([Health Commission of Henan province, 2022](#)). The data include the number of cumulative confirmed cases, daily new pre-symptomatic individuals and the number of daily pre-symptomatic individuals transferred to confirmed cases.

### 2.2. Model

Based on the transmission mechanism, the clinical progress and interventions of the disease, we construct a mathematical model with ordinary differential equations that can represent the overall dynamics of SARS-CoV-2 among people.

In the model, the following assumptions are taken. Since the prevalent period of the epidemic is shorter, the natural birth rate and death rate of human are not taken into account. Meanwhile, since the recovery individuals do not participate in the spread of disease, the group of people are neglected in model. The pre-symptomatic infected people are assumed to have the same infectivity with the infected people at the symptom stage with COVID-19. Infected people who are confirmed and isolated could not infect healthy people and quarantined healthy people can't be infected with COVID-19. The infected people in the latent period will not be detected by nucleic acid testing and do not have the ability to infect other people due to having low viral load in the body. In addition, the interventions taken by the government, including close contact tracking followed by isolation, home quarantine and large-scale nucleic acid testing of non-quarantined population will be incorporated into model. Home quarantine refers to stay at home, while isolation after close contact tracking means being isolated at assigned place which is a more stringent measure. It should be emphasized that large-scale nucleic acid testing measure later in the paper all refers to the detection for non-quarantined population, called as “social testing” in China.

Based on the above assumptions, we subdivide the total human population into eight compartments. That is, the susceptible ( $S$ ), the exposed ( $A$ ), the infected and pre-symptomatic ( $P$ ), the infected with symptoms ( $I$ ), the exposed that are isolated ( $A_q$ ), the pre-symptomatic that are isolated ( $P_q$ ), the cumulative confirmed cases from non-quarantined population ( $C$ ), and the cumulative confirmed cases from isolation people ( $C_q$ ). The flow diagram of the disease transmission among above subpopulations is shown in Fig. 1. The chain in the top half of Fig. 1 with pink background represents the natural transmission processes of the epidemic among non-quarantined population. Susceptible people become exposed people after being infected due to contacting with pre-symptomatic individuals ( $P$ ) or symptomatic individuals ( $I$ ). Let  $\beta$  denotes the effective transmission coefficients of infected individuals. Exposed people develop to pre-symptomatic infected people at a rate coefficient  $m$ , where  $1/m$  is the average latent period. The progression of pre-symptomatic infected individuals to symptomatic infected class is at a rate coefficient  $k$ , where  $1/k$  is the average pre-symptomatic infection period. The epidemic transmission with interventions is shown in the bottom half of Fig. 1 with blue background. A proportion,  $q$ , of infected individuals are isolated through close contact tracking. The isolated individuals move to the compartment  $A_q$ ,  $P_q$  or  $C_q$  at a rate

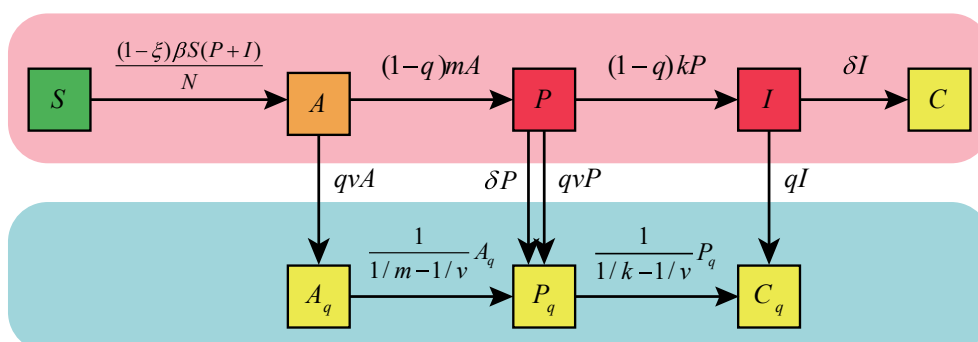


Fig. 1. Flow diagram of COVID-19 model.

$qvA$ ,  $qvP$  and  $qI$  from  $A$ ,  $P$ ,  $I$ , respectively.  $v$  represents the isolation rate coefficient for compartment  $A$  and  $P$ . While the remaining proportion,  $1 - q$  of infected individuals escape from the close contact tracking and develop to the next compartment of epidemiological state according to natural course of disease. Due to home quarantine and static management for city, only susceptible individuals with a fraction  $1 - \xi$  participate in disease transmission.  $\delta$  represents coefficient of detection rate of the infectious individuals to be confirmed to be positive which depends on detection scale and frequency.

The model is given as follows.

$$\begin{cases} \frac{dS}{dt} = \frac{(1-\xi)\beta SP}{N} - \frac{(1-\xi)\beta SI}{N}, \\ \frac{dA}{dt} = \frac{(1-\xi)\beta SP}{N} + \frac{(1-\xi)\beta SI}{N} - (1-q)mA - qvA, \\ \frac{dP}{dt} = (1-q)mA - (1-q)kP - qvP - \delta P, \\ \frac{dI}{dt} = (1-q)kP - \delta I - qI, \\ \frac{dA_q}{dt} = qvA - \frac{1}{1/m - 1/v}A_q, \\ \frac{dP_q}{dt} = qvP + \frac{1}{1/m - 1/v}A_q - \frac{1}{1/k - 1/v}P_q + \delta P, \\ \frac{dC}{dt} = \delta I, \\ \frac{dC_q}{dt} = \frac{1}{1/k - 1/v}P_q + qI. \end{cases} \quad (1)$$

with the nonnegative initial values:

$$S(0) = S_0, A(0) = A_0, P(0) = P_0, I(0) = I_0, A_q(0) = A_{q0}, P_q(0) = P_{q0}, C(0) = C_0, C_q(0) = C_{q0}.$$

Additionally, the total size of the population at time  $t$  is denoted by  $M(t)$ , and  $M = S + A + P + I + A_q + P_q + C + C_q$ , the total size of the population involved in disease transmission at time  $t$  is denoted by  $N(t)$ , and  $N = (1 - \xi)S + A + P + I$ . Adding all eight equations in system (1), we obtain  $dM/dt = 0$ , for all  $t \geq 0$ , which implies  $M(t) = M(0) > 0$  for all  $t \geq 0$ . Then the invariant region for system (1) is

$$\Omega = \{(S, A, P, I, A_q, P_q, C, C_q) \in \mathbb{R}_+^8 : 0 < S, A, P, I, A_q, P_q, C, C_q \leq M\}.$$

### 2.3. Key quantities

We will present the definitions and expressions of the basic reproduction number, transmission rate and controlled rate of the COVID-19 by analyzing model (1). The basic reproduction number is the mean number of secondary cases produced by a single infection in a completely susceptible population during the infection period, which is applied to assess the transmission situation of the epidemic at the initial phase. Applying the next generation matrix theory in (Van den Driessche & Watmough, 2002), we can calculate the basic reproduction number  $R_0 = \rho(FV^{-1})$ , where

$$F = \begin{bmatrix} 0 & \beta & \beta & 0 & 0 \\ 0 & 0 & 0 & 0 & 0 \\ 0 & 0 & 0 & 0 & 0 \\ 0 & 0 & 0 & 0 & 0 \\ 0 & 0 & 0 & 0 & 0 \end{bmatrix}$$

$$V = \begin{bmatrix} (1-q)m + qv & 0 & 0 & 0 & 0 \\ -(1-q)m & (1-q)k + qv + \delta & 0 & 0 & 0 \\ 0 & -(1-q)k & \delta + q & 0 & 0 \\ -qv & 0 & 0 & \frac{1}{1/m - 1/v} & 0 \\ 0 & -qv - \delta & 0 & \frac{-1}{1/m - 1/v} & \frac{1}{1/k - 1/v} \end{bmatrix}$$

Thus

$$\begin{aligned}
R_0 &= \rho(FV^{-1}) \\
&= \frac{\beta(1-q)m[\delta+q+(1-q)k]}{[(1-q)m+qv][(1-q)k+qv+\delta](\delta+q)} \\
&= \beta \frac{(1-q)m}{(1-q)m+qv} \frac{1}{(1-q)k+qv+\delta} + \beta \frac{(1-q)m}{(1-q)m+qv} \frac{(1-q)k}{(1-q)k+qv+\delta} \frac{1}{\delta+q} \\
&\equiv R_p + R_l.
\end{aligned} \tag{2}$$

the basic reproduction number in (2) is composed of two components: secondary infections generated from the infectious people without symptom ( $R_p$ ) and with symptom ( $R_l$ ), respectively.

We define two indices: the transmission rate and the controlled rate, which are important quantities to assess the spread and control level of infectious diseases. Transmission rate ( $v_t$ ) refers to the number of new cases infected with the virus per unit of time. Controlled rate ( $v_c$ ) refers to the number of the infected persons that withdraw from transmission process per unit time under control measures, which is the sum of isolation rate ( $v_i$ ) and detection rate ( $v_d$ ) in this paper. Isolation rate is the number of infected persons isolated per unit of time due to close contact tracking and detection rate is the number of infected persons confirmed per unit of time due to large-scale nucleic acid testing. According to model (1), we give their mathematical expressions:

$$v_t = \frac{(1-\xi)\beta SP}{N} + \frac{(1-\xi)\beta SI}{N}. \tag{3}$$

$$v_i = qvA + qvP + qI, \quad v_d = \delta P + \delta I,$$

so

$$v_c = v_i + v_d = qvA + qvP + qI + \delta P + \delta I. \tag{4}$$

We notice

$$\frac{dA}{dt} + \frac{dP}{dt} + \frac{dI}{dt} = v_t - v_c.$$

From the equation

$$\frac{dA}{dt} + \frac{dP}{dt} + \frac{dI}{dt} = v_t - v_c = 0.$$

We obtain

$$R(t) = \frac{v_t}{v_c},$$

where  $R(t)$  represents the effective reproduction number which means that the average number of secondary infections produced by an infected individual at time  $t$  during the infection period (Cao et al., 2020).

#### 2.4. Parameter estimation approach

The estimation of parameters in this paper is carried out in two steps (de León et al., 2020). First, We use the nonlinear least square method to fit the model with real data. The sum of squared residuals, that is objective function, is defined as:

$$SSE = \sum_{i=1}^n (x_i - \tilde{x}_i(\theta))^2. \tag{5}$$

where  $x_i$  and  $\tilde{x}_i(\theta)$  represent observational data and the solution of the model, respectively.  $\theta$  stands for estimated parameters. The objectives of data fitting are to obtain the values of model parameters  $\theta$  by minimizing the equation (5) and to verify the rationality of the model. Secondly, the Markov Chain Monte Carlo (MCMC) method is adopted to find confidence intervals of estimated parameters  $\theta$ , where Metropolis-Hastings algorithm is used to carry out random sampling. We set 10000 iterations in the MCMC procedure, where the first 9000 are regarded as the burn period. Then we calculate the model solutions under each set of samples of parameters, and the mean and standard deviation of solutions after the burn period. Finally we obtain the mean, standard deviation and 95% confidence interval of the estimated parameters  $\theta$  and the basic reproduction number.

For the Xi'an outbreak, December 15, 2021 is taken as the starting point of the epidemic for fitting and analysis, because the three cases detected before December 15 that belong to the first two chains of transmission respectively didn't cause further spread. For outbreaks in Zhengzhou and Yuzhou in Henan province, the source of infection is unknown. In that case, we need to estimate the length of the concealed transmission period  $t_0$ , i.e. the time between infected first and detected first. For which we give the following approach to handle with.

During the concealed transmission period, the epidemic have not yet been detected and the virus spread naturally in population. Therefore, it is reasonable to assume that parameters which correspond to control measures are equal to 0, i.e  $\xi = \delta = q = v = 0$ . So model (1) is transformed into:

$$\begin{cases} \frac{dS}{dt} = -\frac{\beta SP}{M} - \frac{\beta SI}{M}, \\ \frac{dA}{dt} = \frac{\beta SP}{M} + \frac{\beta SI}{M} - mA, \\ \frac{dP}{dt} = mA - kP, \\ \frac{dI}{dt} = kP. \end{cases} \quad (6)$$

when the number of infected people is relatively small compared with the population size  $M$  at the start of an epidemic in a city, model (6) can be rewritten using  $S \approx M$  as homogeneous linear differential equations. We solve linear differential equations with an initial value  $x_0(M-c, c, 0, 0)$ , which is the value of variables on the day when the first infected person was infected, and  $c$  represents the initial number of infected persons in the concealed transmission period. According to the solution, we obtain the initial value of model (1) ( $S(0), A(0), P(0), I(0)$ ), which is the value of variables on the day when the epidemic was discovered, and estimate the length of the concealed transmission period  $t_0$ :

$$\begin{cases} S(0) = c_1 e^{\lambda_1 t_0} + c_3 \frac{(m-g)(m+g-2k)}{4km} e^{\lambda_3 t_0} + c_4 \frac{-(m+g)(2k+g-m)}{4km} e^{\lambda_4 t_0}, \\ A(0) = c_3 \frac{(m+g)(m+g-2k)}{4km} e^{\lambda_3 t_0} + c_4 \frac{(g-m)(2k+g-m)}{4km} e^{\lambda_4 t_0}, \\ P(0) = c_2 e^{\lambda_2 t_0} + c_3 \frac{-(m+g)}{2k} e^{\lambda_3 t_0} + c_4 \frac{(g-m)}{2k} e^{\lambda_4 t_0}, \\ I(0) = -c_2 e^{\lambda_2 t_0} + c_3 e^{\lambda_3 t_0} + c_4 e^{\lambda_4 t_0}, \end{cases}$$

where

$$\begin{aligned} g &= \sqrt{m(4\beta + m)}; \\ c_1 &= M, c_2 = \frac{2kmc}{g} \left( \frac{1}{2k+g-m} + \frac{1}{m+g-2k} \right), c_3 = \frac{2kmc}{g(m+g-2k)}, c_4 = \frac{2kmc}{g(2k+g-m)}; \\ \lambda_1 &= 0, \lambda_2 = -k, \lambda_3 = -\frac{m+g}{2}, \lambda_4 = -\frac{m-g}{2}. \end{aligned}$$

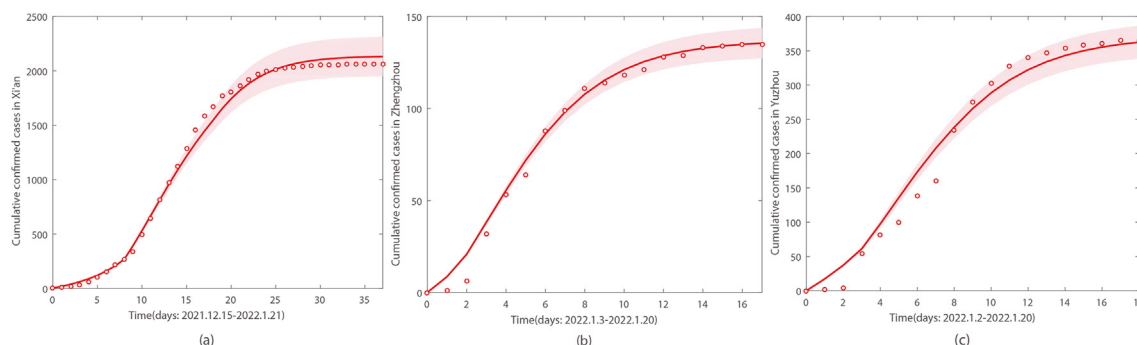


**Fig. 2.** The fitting results of the cumulative number of confirmed cases ( $C+C_q$ ) in Xi'an, Zhengzhou and Yuzhou. Red circles represent the actual cumulative data, the solid red line is the theoretical mean value and the red area represents the 95% confidence interval of 1000 fitting results. The time range of fitting consists of the total time it took for an epidemic from start to finish.

### 3. Results

#### 3.1. Parameter values

We apply the dynamical model (1) to fit the cumulative number of daily confirmed cases of three cities and estimate the values of parameters, respectively. The fitting results are shown in Fig. 2, where the mean value and 95% confidence interval at each time point are contained. The accuracy of the model is also verified.

The parameters values for model corresponding to the fitting curve for three regions are listed in Table 1. The values and sources of partial parameter are interpreted as follows: (1) Parameters  $\xi$  and  $\delta$  alter in time as interventions are implemented and changed. The values of parameter  $\xi$  are reckoned based on the range of controlled zones. The values of parameter  $\delta$  are reckoned based on the cycle of large-scale nucleic acid testing.

The values of parameter  $\xi$  in Xi'an, Zhengzhou and Yuzhou are given as follows, respectively.

$$\xi = \begin{cases} 0.06, & t \in [12.15, 12.22], \\ 0.57, & t \in [12.23, 1.21]. \end{cases}, \xi = 0.07, \quad t \in [1.3, 1.20]. \quad \xi = \begin{cases} 0.24, & t \in [1.2, 1.5], \\ 0.48, & t \in [1.6, 1.20]. \end{cases} \quad (7)$$

The values of parameter  $\delta$  in Xi'an, Zhengzhou and Yuzhou are:

$$\delta = \begin{cases} 0, & t \in [12.15, 12.22], \\ 0.5, & t \in [12.23, 1.1], \\ 1, & t \in [1.2, 1.21]. \end{cases}, \delta = \begin{cases} \frac{1}{3}, & t \in [1.3, 1.5], \\ 1, & t \in [1.6, 1.20]. \end{cases}, \delta = \begin{cases} 0, & t \in [1.2, 1.5], \\ \frac{2}{3}, & t \in [1.6, 1.9], \\ 1, & t \in [1.10, 1.20]. \end{cases} \quad (8)$$

(2) The strains types of viruses in Zhengzhou and Yuzhou are homologous. Therefore, we assume that the value of parameter  $\beta$  in the Yuzhou is equal to that in Zhengzhou. Meanwhile, Zhengzhou and Xi'an are both new first-tier cities with similar capacity to arrange quarantine places, that is concentrated quarantine resources, so we assume that the value of

**Table 1**

Values of parameters for COVID-19 in Xi'an, Zhengzhou and Yuzhou.

Parameters	Xi'an		Source	Zhengzhou		Source	Yuzhou		Source
	Mean	95%CI		Mean	95%CI		Mean	95%CI	
$m$	1/2	—	(Zhang et al., 2020, 2021; Jin et al., 2020)	1/2	—	(Zhang et al., 2020, 2021; Jin et al., 2020)	1/2	—	(Zhang et al., 2020, 2021; Jin et al., 2020)
$k$	1/3	—	(Zhang et al., 2020, 2021; Jin et al., 2020)	1/3	—	(Zhang et al., 2020, 2021; Jin et al., 2020)	1/3	—	(Zhang et al., 2020, 2021; Jin et al., 2020)
$\nu$	1.2072	[1.2071, 1.2073]	MCMC	1.2072	—	Assumed	0.7682	[0.7681, 0.7683]	MCMC
$t_0$	10.5	—	AS	7.7988	[7.7966, 7.8010]	MCMC	8.2700	[8.2655, 8.2745]	MCMC
$c$	2	—	AS	1	—	Assumed	1	—	Assumed
$\xi$	equation (7)	—	AS	equation(7)	—	AS	equation (7)	—	AS
$\delta$	equation (8)	—	AS	equation(8)	—	AS	equation (8)	—	AS
$\beta$	0.7465	[0.7462, 0.7467]	MCMC	1.1923	[1.1921, 1.1925]	MCMC	1.1923	—	Assumed
$q$	0.1629	[0.1627, 0.1631]	MCMC	0.3546	[0.3540, 0.3552]	MCMC	0.4230	[0.4228, 0.4232]	MCMC
$S(0)$	$1.2953 \times 10^7$	—	(Xian Statistics Bureau, 2020)	$1.2601 \times 10^7$	—	(Zhengzhou Statistics Bureau, 2021)	$1.1098 \times 10^6$	—	(Peoples Government of Xuchang City, 2020)
$A(0)$	46.0575	[45.9941, 46.1210]	MCMC	27.6174	[27.5785, 27.6563]	MCMC	36.0005	[35.9142, 41.36.0976]	MCMC
$P(0)$	30.9995	[30.9618, 31.0371]	MCMC	15.4490	[15.4279, 15.4702]	MCMC	20.1330	[20.0821, 20.1840]	MCMC
$I(0)$	21.1547	[21.1315, 21.1779]	MCMC	9.1399	[9.1277, 9.1520]	MCMC	11.9246	[11.8943, 11.9549]	MCMC
$A_q(0)$	15	—	Assumed	1	—	Assumed	2	—	Assumed
$P_q(0)$	21	—	Assumed	1	—	Assumed	21	—	Assumed
$C_q(0)$	0	—	Data	0	—	Data	0	—	Data
$C(0)$	4	—	Data	0	—	Data	0	—	Data

AS: indicates that the parameters depend on the actual situation.



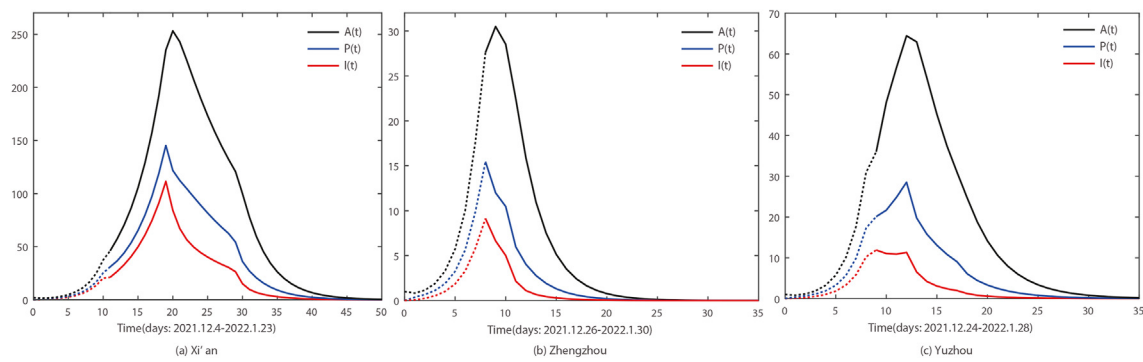


**Fig. 3.** Graphs for the spread of COVID-19 in Xi'an, Zhengzhou and Yuzhou. The dotted lines indicate transmission during concealed transmission period, and the solid lines represent transmission after the outbreak was detected. Black curve shows  $A(t)$ , blue curve shows  $P(t)$  and red curve shows  $I(t)$ .

parameter  $v$  in Zhengzhou is the same as that in Xi'an. (3) The initial number of infected persons in the concealed transmission period is unknown in Zhengzhou and Yuzhou, we assume that  $c = 1$ . (4) The sum of  $a_q(0)$  and  $p_q(0)$  can be obtained through the information of traces. But their respective values are unknown, we make assumption based on the time of diagnosis.

As shown in Table 1, the mean value of the parameter  $t_0$  is 7.7988 in Zhengzhou that shows the outbreak in Zhengzhou originated on December 26, 2021. Similarly, the outbreak in Yuzhou started on December 24, 2021. Therefore, it can be inferred that the outbreak in Yuzhou was prior to Zhengzhou. In fact, we also estimate the length of concealed period ( $t_0$ ) of Xi'an to be 10.5054 with a 95% confidence interval [10.4879, 10.5229], which incorporates the actual length of  $t_0$  10.5. It indicates that our method of estimating  $t_0$  is reasonable and feasible. Fig. 3 shows entire spread situations of COVID-19 including the concealed transmission period. We can see that after the outbreak was detected, the number of the exposed people  $A(t)$  began to decline in Zhengzhou on the second day and in Yuzhou on the fourth day. However, the number of the exposed people  $A(t)$  in Xi'an continued to rise until the tenth day which is one of reasons that Xi'an had a larger final size of infections.

### 3.2. The assessment of interventions

Substituting the parameters values into equation (2) to obtain the basic reproduction number, and corresponding values are shown in Table 2. The basic reproduction number in Zhengzhou is less than one. It is greater than one in Xi'an and Yuzhou. However, the outbreaks were controlled with increased frequency of the large-scale nucleic acid testing. If Xi'an and Yuzhou conducted large-scale nucleic acid testing once every two days ( $\delta = 1/2$ ) when outbreaks were first detected, the basic reproduction number will fall to 0.666 and 0.7395, respectively. It illustrates that the expansion of the large-scale nucleic acid testing can effectively reduce the basic reproduction number and plays an extremely important role in controlling epidemic situation. In addition,  $R_p$  is greater than one in Xi'an and Yuzhou, and  $R_p$  is even much greater than  $R_I$  in Yuzhou, which shows that transmission capacity of pre-symptomatic infectious persons  $P$  cannot be ignored and may even exceeds that of symptomatic infections  $I$ . Therefore, it is particularly significant to detect and isolate  $P$ , while how to find  $P$  as soon as possible is also one of the difficulties in the current COVID-19 prevention and control.

To quantify COVID-19 transmissibility and assess current effectiveness of control measures, we analyse how  $v_t$  and  $v_c$ , which are defined in 2.3 subsection, change over time (Fig. 4). Without implementing control measures,  $v_t$  becomes gradually fast and  $v_c$  is always 0 during the concealed transmission period. As of the day of detection,  $v_t$  in Zhengzhou reached 29 people per day. But there was an astounding 27.5% increase in  $v_t$  in Xi'an and Yuzhou. The three places all took relevant measures to control after the epidemic was detected. However,  $v_c > v_t$  only in Zhengzhou that shows the effectiveness of interventions in Zhengzhou is undoubtedly the best. Xi'an took 8 days to achieve  $v_c > v_t$  twice as long as Yuzhou. Meanwhile, interventions can indirectly curb the transmission rate  $v_t$  by reducing the number of non-quarantined infected people from the expression of  $v_t$ . We also note that  $v_t$  in Xi'an far beyond other two cities with a peak of 3–4 times higher than theirs and when  $v_t$  of Yuzhou

**Table 2**  
The basic reproduction number in Xi'an, Zhengzhou and Yuzhou.

	Xi'an	Zhengzhou	Yuzhou
$R_p$	1.0675 ([1.0670, 1.0680])	0.5249 ([0.5239, 0.5260])	1.0839 ([1.0832, 1.0846])
$R_I$	1.8292 ([1.8256, 1.8327])	0.1644 ([0.1637, 0.1650])	0.4929 ([0.4922, 0.4937])
$R_0$	2.8966 ([2.8926, 2.9006])	0.6893 ([0.6877, 0.6909])	1.5768 ([1.5754, 1.5783])



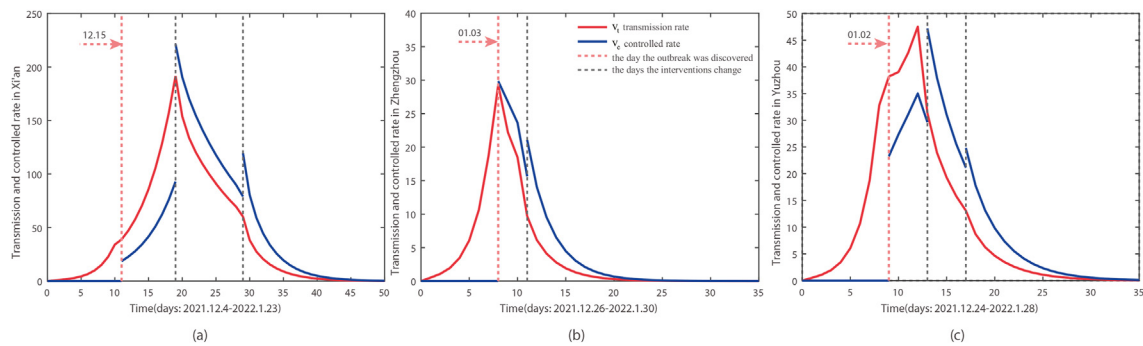


**Fig. 4.** Transmission rate ( $v_t$ ) and controlled rate ( $v_c$ ) in (a) Xi'an, (b) Zhengzhou and (c) Yuzhou. The black dotted lines, as the days on which the interventions change, refer to time nodes when the parameter  $\xi$  in equation (7) and the parameter  $\delta$  in equation (8) change.

had started declining, it continued to rise in Xi'an. Therefore, it illustrates that Xi'an's measures at that time were not enough to control the epidemic. So enhancing interventions is necessary for Xi'an on December 23, 2022.

We provide a sensitivity analysis of incidence  $\frac{(1-\xi)\beta S(P+I)}{N}$  (that is new infected cases per time) with parameters in Xi'an, Zhengzhou and Yuzhou (see Fig. 5) to identify key parameters or control measures that influence the spread of disease by partial rank correlation coefficients (PRCCs) (Wu et al., 2013). We chose a normal distribution for the parameters obtained from MCMC and a uniform distribution for the other parameters. The effect of parameters on incidence varies over time. We observe that: (1) The coefficient of correlation between parameter  $\beta$  and incidence remains above 0.85, showing that measures to reduce the probability of infection such as wearing masks are always effective throughout the entire outbreak. So is the parameter  $q$ , whose coefficient of correlation increases rapidly to  $-0.98$ , almost  $-1$ . Enhancing precision in close contact tracking (increasing  $q$ ) is the most effective control measure. (2) The correlation between the parameters  $\xi$  and incidence is consistently weak, which is almost always around 0. Home quarantine of susceptible people is a weaker measure to reduce the transmission risk of COVID-19. (3) Parameter  $v$  becomes increasingly related with the incidence, especially for Yuzhou, where the correlation increases by up to 48.7%. It confirms that quickening isolation pace (increasing parameter  $v$ ) after close contact tracking is more effective at the late stage of the disease outbreak. And the parameter  $\delta$  shows overall upward trend with oscillation due to the fact that  $\delta$  is piecewise function; (4) In contrast, parameter  $t_0$  becomes less and less relevant to the incidence with time, decreases by 86.2%, 51.5% and 29.5%, respectively. It indicates that discovering outbreak early greatly affects the spread of the disease during the early stage. However, in practice, the first few days after initial infection for COVID-19, individuals may experience no symptoms or unobvious symptom that leads to low desire to seek medical treatment, and hence it will be difficult to diagnose and detect outbreaks as soon as possible. For Zhengzhou and Yuzhou, outbreaks were accidentally discovered when the infected people went to hospital due to other diseases which illustrates the importance of routine nucleic acid testing.

Comparing these three outbreaks, it is found that effective contact coefficients ( $\beta$ ) in Xi'an is the smallest, but its basic reproduction number ( $R_0$ ), the time taken for controlled rate ( $v_c$ ) to exceed transmission rate ( $v_t$ ), duration of the epidemic and final size were the largest. Therefore, it is necessary to retrospectively investigate how to strengthen the control strategy to effectively reduce final size of the epidemic in Xi'an. For this purpose, we discuss the impact of three important parameters  $q$ ,  $v$  and  $\delta$ , that are strongly associated with the incidence (see Fig. 5), on final size of the epidemic in Xi'an by drawing contour plots (see Fig. 6). It follows from Fig. 6 that, increasing  $q$  is more sensitive to reduce the final size than  $\delta_1$ ,  $\delta_2$ ,  $\delta_3$  and  $v$ . When  $q$  is

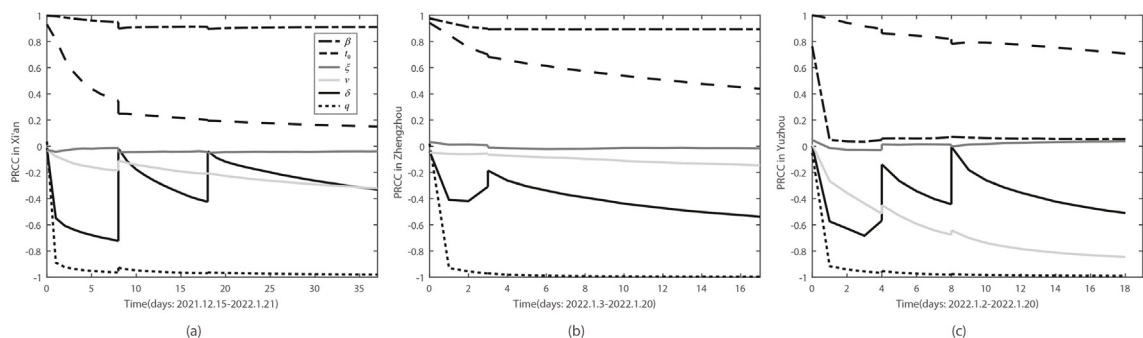


**Fig. 5.** Partial rank correlation coefficients (PRCCs) for the incidence and each input parameter variable. Input parameters are  $\beta$ ,  $t_0$ ,  $\xi$ ,  $v$ ,  $q$ ,  $\delta$ .

sufficiently large (more than 50%), the final size can be reduced by at least 85.39%, even if  $\delta_1$  (or  $\delta_2, \delta_3, v$ ) is in a very small range whose change has little impact on final size, especially  $\delta_2$  and  $\delta_3$ . If  $q$  is very small (less than 5%), it is impossible to control the epidemic with a small final size that is no more than 5000 no matter what are the values  $\delta_2, \delta_3$  and  $v$  (see Fig. 6(b)(c)(d)). However, it doesn't mean that increasing  $\delta_2$  and  $\delta_3$  are unnecessary. It is worth noting that the influence of  $\delta_2$  and  $\delta_3$  on final size increases with decrease of  $q$ , while  $v$  is opposite. All these reflect that enhancing precision in close contact tracking is the most valid method in view of the circumstance in Xi'an. Furthermore, if close contact tracking is wear, intensifying large-scale nucleic acid testing is effective (see Fig. 6(e)(f)(g)). We find that increasing  $\delta_1$  is the most effective for decreasing final size followed by  $\delta_2, \delta_3$  and  $v$ . For example, if  $q, \delta_1, \delta_2, \delta_3$  and  $v$  increase by 0.1 respectively, the final size will decrease respectively 63.63%, 33.98%, 13.3%, 0.93% and 10.27%. It indicates that enhancing large-scale nucleic acid testing strategy in the early stages is more effective in reducing the total number of infections, while test in the later period has limited effect on reducing final size since the potential infected people have been quarantined. Therefore, the most stringent testing should be implemented as soon as possible in the early days of the outbreak. However, Xi'an did not pay attention to testing in the early stage, whose large-scale nucleic acid testing strategy was gradually strengthened. As can be seen in Fig. 6(e), the final size of the epidemic could not be reduced to less than 1000, no matter how hard Xi'an tested in the middle and late period. On the contrary, if large-scale nucleic acid testing was implemented in Xi'an at the early stage ( $\delta_1 = 0.5$ ), the final size would be reduced to 412, with a decline rate of 79.93%.

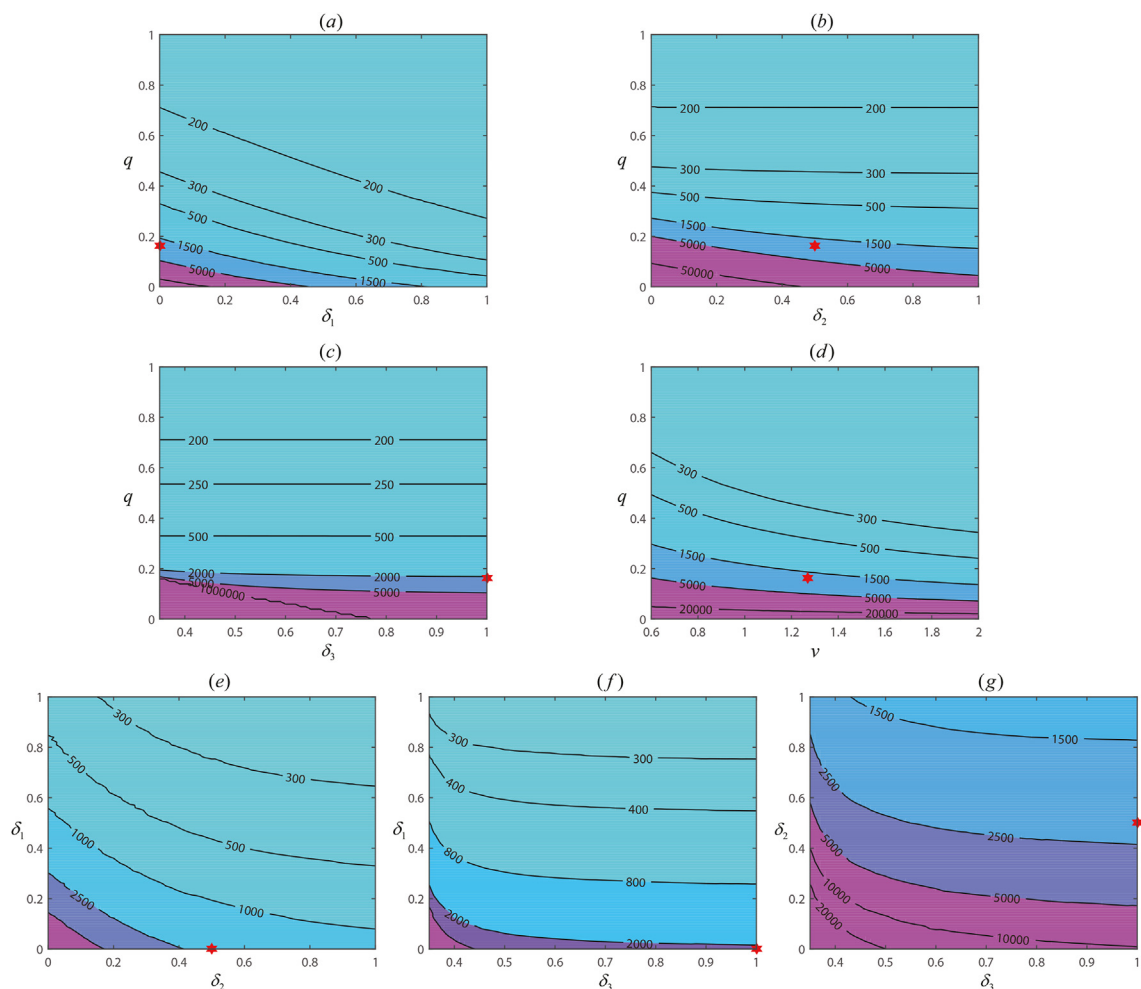


**Fig. 6.** Contour plots of final size of the epidemic in Xi'an. The red hexagon represents the actual situation in Xi'an.  $\delta_1$  indicates earlier coefficient of detection rate (2021.12.15–2021.12.22),  $\delta_2$  is the medium-term coefficient of detection rate (2021.12.23–2022.1.1) and  $\delta_3$  shows later coefficient of detection rate (2022.1.2–2022.1.21).

#### 4. Discussion and conclusions

There are different final size for local COVID-19 outbreaks in China, even as similar interventions and policy are adopted. So it is essential to explore effectiveness of control measures to prevent large-scale outbreaks of COVID-19. Therefore, we establish a mathematical model with mass testing and quarantine measures to compare the local outbreaks in Xi'an, Zhengzhou and Yuzhou to explore internal transmission and control mechanism.

First, we verify the model with the cumulative number of daily confirmed cases and estimate the model parameters in three cities. The beginning time of the epidemic is estimated, and entire spread process of COVID-19 with time is deduced, especially in concealed transmission period. In order to reflect the transmission capacity of the epidemic and the implementation and effect of intervention measures, we obtain the basic reproduction number  $R_0$  of COVID-19 by the next generation matrix method.  $R_0$  in Xi'an equals to 2.5421 that is greater than Zhengzhou and Yuzhou. Meanwhile, transmission rate ( $v_t$ ) in Xi'an is larger. It was 191 on December 22, 2021 which was 3–4 times more than other two cities. And controlled rate ( $v_c$ ) didn't catch up with  $v_t$  until the eighth day after the disease was discovered. All these mean that the epidemic is more serious and the overall effect of the intervention is smaller in Xi'an, which cause that the final size in Xi'an is the largest among the three cities.

To further investigate what caused the epidemic in Xi'an to be more severe than in the other two cities, we evaluate the effect of each intervention on controlling epidemic situation through sensitivity analysis. The analysis based on PRCCs shows that the key variables that contribute to new daily infections are those associated with close contact tracking, large-scale nucleic acid testing and transmission probability. Comparing these measures in the three cities, we find that the effective contact coefficients ( $\beta$ ) of Xi'an is the lowest among three places. However, the precision in close contact tracking ( $q$ ) is also the lowest in Xi'an followed by Zhengzhou, Yuzhou. This may be because Yuzhou, as a prefectural class town, has a simple contact network among people than the other two cities. Hidden transmission in the community in Xi'an has greatly increased the difficulty of tracking. For large-scale nucleic acid testing ( $\delta$ ), the speed and frequency of implementation in the early days arrange from low to high as: Xi'an, Yuzhou and Zhengzhou. Xi'an did not immediately carry out testing after the epidemic was discovered, while the two cities of Zhengzhou and Yuzhou learned from Xi'an and tried their best to carry out large-scale testing when the outbreak was discovered. In addition, perhaps there are fewer places in Yuzhou to isolate close contacts than in the other two cities, resulting in the slowest isolation pace after close contact tracking ( $v$ ).

With all that said, Xi'an had the lowest probability of infection, but the mass tracking and testing strategies were not fully implemented, resulting in the worst effect of comprehensive intervention and the largest final size. Further, we draw Contour plots to explore how to reduce final size of Xi'an. We find that large-scale nucleic acid testing strategy in early period works better than middle and late phases. If Xi'an conducts test once every two days in the early stage as it does in the middle stage, the final size will be reduced by at least 75%. Of course, strengthening testing strategy in the middle and late period also made a certain contribution to contain the epidemic, otherwise it will lead more than 20,000 people to be infected. We also point out that enhancing the precision of close contact tracking is more effective than large-scale nucleic acid testing. For example, if the tracking accuracy is increased to 0.5, the final size of the epidemic in Xi'an will not exceed 300.

In summary, we find that the mass tracking and testing strategies are most effective, which is consistent with (Djaoue et al., 2020; Li et al., 2021). However, the differences from the previous studies are that we further get that large-scale nucleic acid testing is not essential when the close contact tracking is strictly implemented. We also develop a method to estimate the length of the concealed period and the transmission process during the period, define two new indicators to evaluate the effectiveness of the interventions in real time, and eventually reveal the cause of the severity of the outbreak in Xi'an.

The model presented in this paper not only is applicable for the three cases studied, Xi'an, Zhengzhou and Yuzhou, but other regions in China during the implementation of mass tracking and testing strategies as well. Therefore, this study provides information on the design and evaluation of interventions in China. In addition, we do not consider the role of vaccine coverage and protection rate in controlling the outbreak. Considering the effect of vaccines will make the model more complex and have more parameters, which is our future work.

#### Funding

This work is supported by Fund Program for the Scientific Activities of Selected Returned Overseas Professionals in Shanxi Province (20210009), the National Natural Science Foundation of China under Grant (11801398), the 1331 Engineering Project of Shanxi Province, Key Projects of Health Commission of Shanxi Province (No. 2020XM18), and the Key Research and Development Project in Shanxi Province (202003D31011/GZ).

#### Authors contributions

X.W., J.Z., M.L., X.P., and Z.L. determined the research theme, conceived and designed the research methods. X.W. and J.Z. carried out data analysis, programming and wrote the paper. All authors gave final approval for publication.

#### Declaration of competing interest

The authors declare that they have no competing interests.

## References

- Biala, T., Afolabi, Y., & Khaliq, A. (2022). How efficient is contact tracing in mitigating the spread of covid-19? A mathematical modeling approach. *Applied Mathematical Modelling*, 103, 714–730. <https://doi.org/10.1016/j.apm.2021.11.011>
- Cao, Z., Zhang, Q., Lu, X., Pfeiffer, D. U., Jia, Z., Song, H., & Zeng, D. D. (2020). Estimating the effective reproduction number of the 2019-ncov in China. *medRxiv*. <https://doi.org/10.1101/2020.01.27.20018952>
- Ceraolo, C., & Giorgi, F. M. (2020). Genomic variance of the 2019-ncov coronavirus. *Journal of Medical Virology*, 92(5), 522–528. <https://doi.org/10.1002/jmv.25700>
- Chinese State Council (2020). (2020). Chinas action to fight the covid-19 epidemic. [http://www.gov.cn/zhengce/2020-06/07/content\\_5517737.htm](http://www.gov.cn/zhengce/2020-06/07/content_5517737.htm). (Accessed 13 October 2022).
- Djaoue, S., Kolaye, G. G., Abboubakar, H., Ari, A. A. A., & Damakoa, I. (2020). Mathematical modeling, analysis and numerical simulation of the covid-19 transmission with mitigation of control strategies used in Cameroon. *Chaos, Solitons & Fractals*, 139, Article 110281. <https://doi.org/10.1016/j.chaos.2020.110281>
- Health Commission of Henan province. (2022). <https://wsjkw.henan.gov.cn/>. (Accessed 13 October 2022).
- Health Commission of Shaanxi province. (2022). <http://sxwjw.shaanxi.gov.cn/>. (Accessed 13 October 2022).
- Hui, D. S., Azhar, E. I., Madani, T. A., Ntoumi, F., Kock, R., Dar, O., et al. (2020). The continuing 2019-ncov epidemic threat of novel coronaviruses to global health the latest 2019 novel coronavirus outbreak in wuhan, China. *International Journal of Infectious Diseases*, 91, 264–266. <https://doi.org/10.1016/j.ijid.2020.01.009>
- Jin, X., Lian, J.-S., Hu, J.-H., Gao, J., Zheng, L., Zhang, Y.-M., et al. (2020). Epidemiological, clinical and virological characteristics of 74 cases of coronavirus-infected disease 2019 (covid-19) with gastrointestinal symptoms. *Gut*, 69(6), 1002–1009. <https://doi.org/10.1136/gutjnl-2020-320926>
- Khairulbahri, M. (2021). Lessons learned from three southeast asian countries during the covid-19 pandemic. *Journal of Policy Modeling*, 43(6), 1354–1364. <https://doi.org/10.1016/j.jpolmod.2021.09.002>
- Kondo, K. (2021). Simulating the impacts of interregional mobility restriction on the spatial spread of covid-19 in Japan. *Scientific Reports*, 11(1), 1–15. <https://doi.org/10.1038/s41598-021-97170-1>
- de León, U. A.-P., Pérez, Á. G., & Avila-Vales, E. (2020). An seiard epidemic model for covid-19 in Mexico: Mathematical analysis and state-level forecast. *Chaos, Solitons & Fractals*, 140, Article 110165. <https://doi.org/10.1016/j.chaos.2020.110165>
- Li, F., Jin, Z., & Zhang, J. (2021). Assessing the effectiveness of mass testing and quarantine in the spread of covid-19 in beijing and xinjiang, 2020. *Complexity*, 2021. <https://doi.org/10.1155/2021/5510428>
- Liu, W., Guo, Z., Abudunaibi, B., Ouyang, X., Wang, D., Yang, T., et al. (2022). Model-based evaluation of transmissibility and intervention measures for a covid-19 outbreak in xiamen city, China. *Frontiers in Public Health*, 1858. <https://doi.org/10.3389/fpubh.2022.887146>
- Maged, A., Ahmed, A., Haridy, S., Baker, A. W., & Xie, M. (2022). Seir model to address the impact of face masks amid covid-19 pandemic. *Risk Analysis*. <https://doi.org/10.1111/risa.13958>
- Majumder, M., Tiwari, P. K., & Pal, S. (2022). Impact of saturated treatments on hiv-tb dual epidemic as a consequence of covid-19: Optimal control with awareness and treatment. *Nonlinear Dynamics*, 1–34. <https://doi.org/10.1007/s11071-022-07395-6>
- Peoples Government of Xuchang City. (2020). The 7th national population census bulletin of xuchang. <http://www.xuchang.gov.cn/openDetailDynamic.html?infoId=b7aba810-8676-4cbe-9cdd-87e5d2ee8655>. (Accessed 13 October 2022).
- Qi, Z., & Yu, Y. (2020). Epidemiological features of the 2019 novel coronavirus outbreak in China. *Current Topics in Medicinal Chemistry*, 20(13), 1137–1140. <https://doi.org/10.2174/1568026620999200511094117>
- Rai, R. K., Khajanchi, S., Tiwari, P. K., Venturino, E., & Misra, A. K. (2022). Impact of social media advertisements on the transmission dynamics of covid-19 pandemic in India. *Journal of Applied Mathematics and Computing*, 68(1), 19–44. <https://doi.org/10.1007/s12190-021-01507-y>
- Saadatmand, S., Salimifard, K., & Mohammadi, R. (2022). Analysis of non-pharmaceutical interventions impacts on covid-19 pandemic in Iran. *Nonlinear Dynamics*, 109, 225–238. <https://doi.org/10.1007/s11071-021-07121-8>
- Song, H., Jia, Z., Jin, Z., & Liu, S. (2021). Estimation of covid-19 outbreak size in harbin, China. *Nonlinear Dynamics*, 106(2), 1229–1237. <https://doi.org/10.1007/s11071-021-06406-2>
- Song, H., Li, F., Jia, Z., Jin, Z., & Liu, S. (2020). Using traveller-derived cases in henan province to quantify the spread of covid-19 in wuhan, China. *Nonlinear Dynamics*, 101(3), 1821–1831. <https://doi.org/10.1007/s11071-020-05859-1>
- Sun, G.-Q., Ma, X., Zhang, Z., Liu, Q.-H., & Li, B.-L. (2022). What is the role of aerosol transmission in sars-cov-2 omicron spread in shanghai? *BMC Infectious Diseases*, 22(1), 1–15. <https://doi.org/10.1186/s12879-022-07876-4>
- Sun, G.-Q., Wang, S.-F., Li, M.-T., Li, L., Zhang, J., Zhang, W., Jin, Z., & Feng, G.-L. (2020). Transmission dynamics of covid-19 in wuhan, China: Effects of lockdown and medical resources. *Nonlinear Dynamics*, 101(3), 1981–1993. <https://doi.org/10.1007/s11071-020-05770-9>
- Tang, B., Wang, X., Li, Q., Bragazzi, N. L., Tang, S., Xiao, Y., & Wu, J. (2020). Estimation of the transmission risk of the 2019-ncov and its implication for public health interventions. *Journal of Clinical Medicine*, 9(2), 462. <https://doi.org/10.3390/jcm9020462>
- Tiwari, P. K., Rai, R. K., Khajanchi, S., Gupta, R. K., & Misra, A. K. (2021). Dynamics of coronavirus pandemic: Effects of community awareness and global information campaigns. *The European Physical Journal Plus*, 136(10), 994. <https://doi.org/10.1140/epjp/s13360-021-01997-6>
- Van den Driessche, P., & Watmough, J. (2002). Reproduction numbers and sub-threshold endemic equilibria for compartmental models of disease transmission. *Mathematical Biosciences*, 180(1–2), 29–48. [https://doi.org/10.1016/S0025-5564\(02\)00108-6](https://doi.org/10.1016/S0025-5564(02)00108-6)
- Wang, X.-L., Lin, X., Yang, P., Wu, Z.-Y., Li, G., McGoogan, J. M., et al. (2021). Coronavirus disease 2019 outbreak in beijings xinfadi market, China: A modeling study to inform future resurgence response. *Infectious diseases of poverty*, 10(1), 1–10. <https://doi.org/10.1186/s40249-021-00843-2>
- Wang, Q., Xie, S., Wang, Y., & Zeng, D. (2020). Survival-convolution models for predicting covid-19 cases and assessing effects of mitigation strategies. *Frontiers in Public Health*, 325. <https://doi.org/10.1101/2020.04.16.20067306>
- World Health Organization. (2020). Who director-generas opening remarks at the media briefing on covid-19- 11 march 2020. <https://www.who.int/zh/director-general/speeches/detail/who-director-general-s-opening-remarks-at-the-media-briefing-on-covid-19%2D%2D-11-March-2020>. (Accessed 13 October 2022).
- World Health Organization. (2022). Cweekly epidemiological update on covid-19 - 5 october 2022. <https://www.who.int/publications/m/item/weekly-epidemiological-update-on-covid-19&mdash;5-october-2022>. (Accessed 13 October 2022).
- Wu, J., Dhingra, R., Gambhir, M., & Remais, J. V. (2013). Sensitivity analysis of infectious disease models: Methods, advances and their application. *Journal of The Royal Society Interface*, 10. <https://doi.org/10.1098/rsif.2012.1018>
- Xian Statistics Bureau. (2020). Statistics on land area and density of permanent population (2020). <http://tjj.xa.gov.cn/tjnj/2021/zk/indexch.htm>. (Accessed 13 October 2022).
- Yang, T., Wang, Y., Liu, N., Abudurusuli, G., Yang, S., Yu, S., et al. (2022). Modeling cross-regional transmission and assessing the effectiveness of restricting inter-regional population movements in controlling covid-19xian city, shaanxi province, China, 2021. *China CDC Weekly*, 4(31), 685–692. <https://doi.org/10.46234/ccdcw2022.143>
- Yu, Y., Zhou, Y., Meng, X., Li, W., Xu, Y., Hu, M., & Zhang, J. (2021). Evaluation and prediction of covid-19 prevention and control strategy based on the seir-aq infectious disease model. *Wireless Communications and Mobile Computing*, 2021. <https://doi.org/10.1155/2021/1981388>

- Zhang, J., Litvinova, M., Wang, W., Wang, Y., Deng, X., Chen, X., et al. (2020). Evolving epidemiology and transmission dynamics of coronavirus disease 2019 outside hubei province, China: A descriptive and modelling study. *The Lancet Infectious Diseases*, 20, 793–802. [https://doi.org/10.1016/S1473-3099\(20\)30230-9](https://doi.org/10.1016/S1473-3099(20)30230-9)
- Zhang, R., Wang, Y., Lv, Z., & Pei, S. (2022). Evaluating the impact of stay-at-home and quarantine measures on covid-19 spread. *BMC Infectious Diseases*, 22(1), 1–13. <https://doi.org/10.1186/s12879-022-07636-4>
- Zhang, M., Xiao, J., ping Deng, A., Zhang, Y., Zhuang, Y., Hu, T., et al. (2021). Transmission dynamics of an outbreak of the covid-19 delta variant b.1.617.2 guangdong province, China, mayjune 2021. *China CDC Weekly*, 3, 584–586. <https://doi.org/10.46234/ccdcw2021.148>
- Zhao, S., Tang, B., Musa, S. S., Ma, S., Zhang, J., Zeng, M., et al. (2021). Estimating the generation interval and inferring the latent period of covid-19 from the contact tracing data. *Epidemics*, 36, Article 100482. <https://doi.org/10.1016/j.epidem.2021.100482>
- Zhengzhou Statistics Bureau. (2021). *The 7th national population census bulletin of zhengzhou (no.2)*. <https://tjj.zhengzhou.gov.cn/tjgb/5012682.jhtml>. (Accessed 13 October 2022).